J. Chem. Sci. (2020)132:30
https://doi.org/10.1007/s12039-019-1721-7

REGULAR ARTICLE

Diphenyl phosphate creatine immobilized on magnetite nanoparticles: an efficient and recyclable catalyst for Aza-Michael reaction

FARZANE PAZOKI, FAHIMEH MOHAMMADPANAH, AREFE SALAMAT MANESH, JAMSHID AZARNIA MEHRABAN and AKBAR HEYDARI*
Department of Chemical, Faculty of Sciences, Tarbiat Modares University, Tehran 14117-13116, Iran
E-mail: HEYDAR_A@modares.ac.ir
This article is dedicated to the memory of Mohammad-li Rajai.

MS received 14 July 2019; revised 6 September 2019; accepted 19 September 2019

Abstract. In this paper, diphenyl phosphate creatine was successfully immobilized on Fe_3O_4 nanoparticles and used as the highly efficient catalyst for the aza-Michael reaction of 5-substituted tetrazole and α,β-unsaturated carbonyl. The prepared nanocatalyst was fully analyzed by various techniques such as Fourier-transform Infrared Spectroscopy (FT-IR), Field Emission Scanning electron microscope (FE-SEM), Vibrating Sample Magnetometer (VSM), Thermal Gravimetric Analysis (TGA) and X-ray Diffraction (XRD). This procedure possesses numerous advantages such as simple work-up, high yield and short reaction times.

Keywords. Aza-Michael reaction; Diphenyl phosphate Creatine; Tetrazoles; Heterogeneous Catalyst.

1. Introduction

Tetrazoles are a class of important heterocyclic compounds because these compounds have been applied in major areas of science, such as medicine, chemistry and material sciences. Thus, many synthetic methods have been reported for the synthesis of tetrazoles.[1–5] N-functionalization of tetrazoles is an approach for the synthesis of various tetrazole derivatives.[6] The aza-Michael addition of these tetrazoles to α, β-unsaturated carbonyl compounds is a convenient and powerful method to functionalize tetrazoles. There are few reports for this method.[7–10]

Phosphoramides play an important role in many biological processes.[11–15] On the other hand, creatine and phosphate creatine play a key role in fluctuating energy demands, energy transduction in tissues.[16] Considering these facts, diphenyl phosphate creatine can act as chemical and biochemical catalysts due to Diphenyl phosphate creatine is a type of Phosphoramides with substitution of creatine.

Nanomagnetic materials have attended great attention owing to their several applications in synthesis and catalysis.[17,18] The surface of magnetic nanoparticles can be functionalized with various kinds of organic compound.[19] Hence, modified magnetite nanoparticles have attracted as catalytic systems in various organic reactions. They have numerous benefits involving their ease separation, recyclability, excellent chemical stability, good accessibility, high surface, simple preparation, reasonable price and ability to be functionalized.[20–23] In continuation of our efforts to develop simple protocols for the synthesis of tetrazoles[24] and considering the importance of the catalytic activity of diphenyl phosphate creatine, herein, we report successfully synthesis of diphenyl phosphate creatine and Fe_3O_4@Diphenyl phosphate creatine nanoparticles as a green catalyst. In addition, the catalytic performance of synthesized nanoparticles has been investigated in aza- Michael reaction of 5-substituted tetrazole with α, β- unsaturated carbonyl which obtained products in good yields. These magnetically retrievable nanoparticles are highly efficient, environmentally friendly and novel heterogeneous catalyst. The Fe_3O_4@Diphenyl phosphate creatine

*For correspondence

Electronic supplementary material: The online version of this article (https://doi.org/10.1007/s12039-019-1721-7) contains supplementary material, which is available to authorized users.

Published online: 25 January 2020

nanoparticles can be easily separated by an external magnet and their catalytic activity remains unaltered after 6 consecutive cycles. The structure of the nanoparticles was fully characterized by useful analyses. The Fe_3O_4@Diphenyl phosphate creatine nanocatalyst exhibits attractive catalytic efficiency for the aza-Micheal reaction between 5-substituted tetrazole derivatives and α, β-unsaturated carbonyl to synthesize tetrazole derivatives in good yields (Scheme 1).

2. Experimental

2.1 *General considerations*

Chemical materials were purchased from Sigma-Aldrich or Merck. The monitoring of reaction progress was carried out by analytical Thin Layer Chromatography (TLC) on Merck 0.2 mm of silica gel 60F-254 Al-plates. FT-IR was determined on a Shimadzu FT-IR-8400S spectrometer by using the KBr plate technique. ^{1}H NMR (500 MHz) spectra were obtained on Bruker DRX-500 Advance spectrometers with $CHCl_3$ as solvent at ambient temperature using TMS as the internal standard. XRD was carried out by a Philips X-Pert 1710 diffractometer and also SEM was performed on Zeiss-Sigma VP 500. The magnetic measurements experiments were obtained by using a vibrating magnetometer/alternating gradient force magnetometer (MD Co., Iran, www.mdk-magnetic.com).

2.2 *Synthesis*

2.2a *Synthesis of diphenyl phosphate creatine* The methylguanidoacetic acid (15 mmol) and triethylamine (Et_3N, 15 mmol) were dissolved in acetonitrile solvent at −8 °C. Then, 15 mmol of the diphenyl phosphinic chlorophosphate was added drop by drop to the mixture for 30 min. Next, the mixture was stirred for 8 h at 25 °C. Finally, the final product was extracted by water and ethyl acetate.

2.2b *Synthesis of Fe_3O_4@Phenyl phosphate creatine* Fe_3O_4 was prepared by coprecipitation technique.[25] Thus, $FeCl_2.4H_2O$ (0.0216 mol)) and $FeCl_3.6H_2O$ (0.0108 mol) salts were dissolved in deionized water (100 mL) at 25 °C. Afterwards, 10 mL of 25% NH_4OH solution was added drop by drop to the stirring suspension at 25 °C (until pH = 11). Then, diphenyl phosphate creatine (2.5 mmol) was added to this mixture. The resultant nanoparticles were stirred for 1 h at 25 °C and the mixture was heated for 5 h at 80 °C. The final product was separated by an external magnet and washed with deionized water and ethanol three times and dried at 60 °C for 12 h.

2.2c *General procedure for the aza- Michael reaction* A round-bottomed flask (25 mL) was charged with 5-substituted tetrazole derivatives (2.0 mmol), α, β-unsaturated carbonyl (2.0 mmol) and the catalyst (50.0 mg) in methanol (10 mL). The mixture was stirred at 65 °C to reaction completion. After completion, the magnetic nanocatalyst was easily collected by an external magnet. Then, the product was purified by column chromatography, after the product was washed with hexane and diethyl ether three times.

2.3 *Representative spectral data*

2.3a *Diphenyl phosphate creatine* Yield: 73%. M.p.: 14 °C; ^{31}P NMR (202.46 MHz, d6- DMSO, ppm): δ -11.24 (s). ^{1}H NMR (500.13 MHz, d6- DMSO, ppm): δ 13.3 (s, 1H, OH), 7.62 (s, 2H, NH amine), 6.97(t, 3JHH = 9.5 Hz, 2HPh), 7.12 (d, 3JHH = 5 Hz, 4HPh), 7.19 (t, 3 JHH = 7.4 Hz, 4HPh), 4.13 (s, 2H, CH_2), 2.48 (s, 3H, CH_3). ^{13}C NMR (DMSO-d): δ = 41.07(CH_2), 38.78 (CH_3), 119.61, 122.94, 129.9, 1 4.21 (Cipso), 1 7.87(C=N), 1 9.83 (C=O) ppm. IR (KBr, cm^{-1}): 3367 (Vs), 3185 (vs, N–H), 1718(s, C=O), 1667 (s), 1608 (s), 1407 (m), 1211 (vs, P=O), 1100 (m, P–N), 854 (m), 600 (m).

2.3b *Phenyl-1H-tetrazol-1-yl) cyclohexenone (compound 4)* White solid. M.p.: 186–189 °C; ^{1}H NMR (300 MHz, Chloroform-d) δ 2.0–2.16 (m, 2H), 2.32–2.46 (m, 2H), 2.48–2.55 (m, 2H), 2.96–3.22 (m, 2H), 5.15–5.30 (tt, *J* = 9.5, 4.8 Hz,1H), 7.43–7.52 (m, *J* = 4.1, 1.6 Hz, 3H), 8.09–8.21 (m, 2H).^{13}C NMR (75 MHz, $CDCl_3$) δ 21, 31, 40, 4, 1, 12 .8, 127, 129, 130, 1, 20 . IR (KBr) cm^{-1}: 3063 (CH), 1717 (C=O), 1527 (N=N). HRMS (ESI) ([M+H] +) Calcd. For C13H14N4O:242.28, Found: 243.2.

2.3c *benzo[d] [1, 3] dioxol-6-yl)-1H-tetrazol-1-yl) cyclohexenone (compound 6)* White solid. M.p.: 194–195 °C; ^{1}H NMR (300 MHz, Chloroform-*d*) δ 1.89–2.17 (m, 2H), 2.28–2.61 (m, 4H), 2.86–3.26 (m, 2H), 5.17–5.28 (tt, *J* = 9.7, 4.9 Hz, 1H), 5.96–6.14 (s, 2H), 6.91–7.01 (d, *J* = 8.1 Hz, 1H), 7.55–7.66 (d, *J* = 1.6 Hz, 1H), 7.69–7.81 (dd, *J* = 8.1,1.7 Hz, 1H). IR (KBr) cm^{-1}: 1676

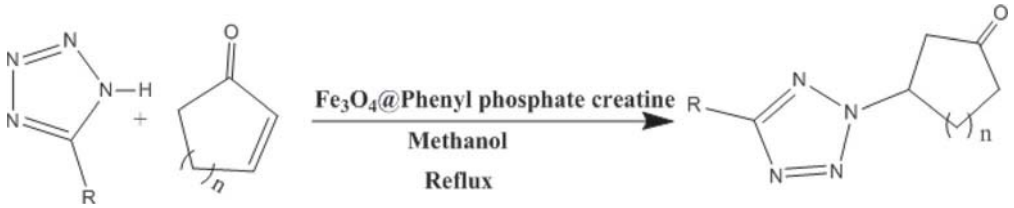

Scheme 1. Catalytic applicability of the Fe_3O_4@Phenyl phosphate creatine.

(C=O), 1599 (N=N), 1451 (C=C), 1383 (C=N). HRMS (ESI) ([M+H] +) Calcd. For $C_{14}H_{13}N_4O_3$:286.11, Found: 286.1

All the synthesized compounds (**1**–**9**) were characterized by ^{1}H, ^{13}C, NMR and IR spectroscopy (see supplementary information).

3. Results and Discussion

Figure 1 shows the FT-IR of the diphenyl phosphate creatine (black curve), Fe_3O_4 (red curve) and Fe_3O_4@Diphenyl phosphate creatine before (blue curve) and after reaction (yellow curve). The FT-IR spectra of diphenyl phosphate creatine (black curve), the peak at 1718 cm^{-1} can be attributed to C=O stretching vibration. The peaks at 1673.9 cm^{-1}, 1596.7 cm^{-1} can be attributed to C=N stretching vibration and the peaks at the near region from 3300 cm^{-1} to 3400 cm^{-1} are assigned to vibrations characteristic of the carboxylic acid. The peak at 1100 cm^{-1} can be attributed to the P–O vibration, these results confirm the formation of phosphate creatine.

In the case of Fe_3O_4 (red curve), the peak at the near region from 3400 cm^{-1} to 3410 cm^{-1} in the curve is assigned to O-H vibrations of water and the absorption peak observes at 578 cm^{-1} due to the Fe–O vibration related to the Fe_3O_4 sample. This result strongly supports the assignment of the synthesized Fe_3O_4.[26]

In the case of Fe_3O_4@Diphenyl phosphate creatine (blue curve), peaks at 1643 cm^{-1}, 1589 cm^{-1} can be assigned to C=N stretching vibration, the absorption peak at 1100 cm^{-1} corresponds to the P–O vibration and the peak observes at 593 cm^{-1} due to the Fe–O vibration. It also shows that the Fe_3O_4@Diphenyl phosphate creatine nanoparticles have the same structure after 6 cycles and this the structure is stable.

The size and structure of the Fe_3O_4@Diphenyl phosphate creatine are estimated by using an FE-SEM (Figure 2). This image showed that prepared nanoparticles have a nearly spherical morphology and the Fe_3O_4@Diphenyl phosphate creatine nanoparticles have a diameter of about 100 nm.

The magnetic properties of Fe_3O_4@Diphenyl phosphate creatine were characterized by VSM at room temperature (Figure 3). The saturation magnetization of Fe_3O_4@Diphenyl phosphate creatine is around 66.1 emu/g which accounts for easy recovery of this catalyst and the magnetization curve demonstrate that these Fe_3O_4@Diphenyl phosphate creatine nanoparticles have superparamagnetic properties.

The XRD diagrams of the Diphenyl phosphate creatine (Black curve), Fe_3O_4 (Red curve) and Fe_3O_4@Diphenyl phosphate creatine (Blue curve) are given in Figure 4. The XRD pattern of Fe_3O_4@-Diphenyl phosphate creatine revealed five reflection peaks (2θ = 35.23°, 41.59°, 50.79°, 67.71°, 74.55°) that indexed as {311}, {400}, {422}, {511} and {440} the XRD peaks are in good agreement with crystalline structure of Fe_3O_4 and these confirmed the formation Fe_3O_4 phase (JCPDS 19-629). And the amount of Diphenyl phosphate creatine supported on magnetic is little therefore we show no obvious peaks of Diphenyl phosphate creatine in XRD diagrams of Fe_3O_4@-Diphenyl phosphate creatine.

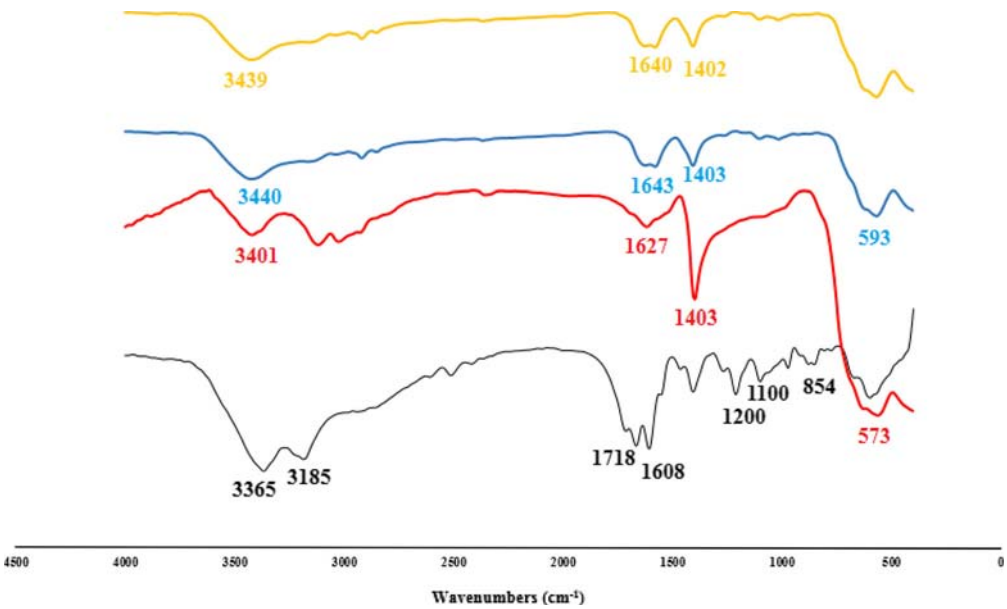

Figure 1. FT-IR spectra of Diphenyl phosphate creatine (black curve), Fe_3O_4 (red curve) and Fe_3O_4@Diphenyl phosphate creatine before (blue curve) and after reaction (yellow curve).

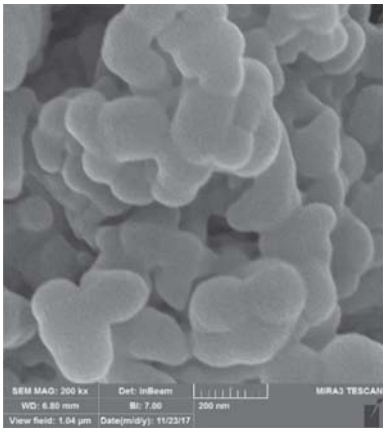

Figure 2. FE-SEM micrographs of Fe_3O_4@Diphenyl phosphate creatine.

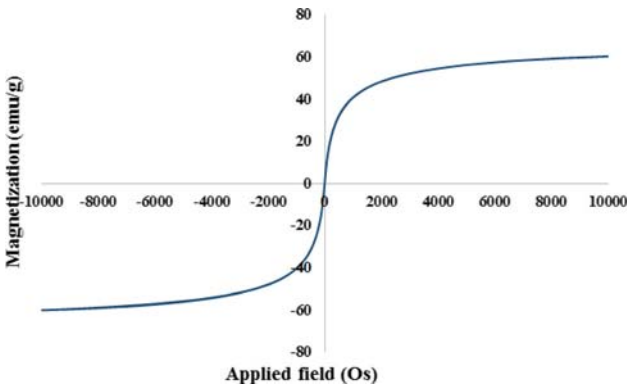

Figure 3. Hysteresis loops of Fe_3O_4@Diphenyl phosphate creatine.

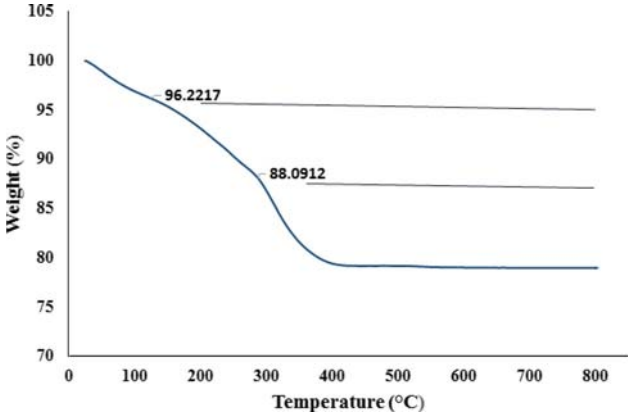

Figure 5. TGA of Fe_3O_4@Diphenyl phosphate creatine.

Thermogravimetric analysis of the nanoparticles was used for investigation of the per cent of organic functional groups chemisorbed onto the surface of Fe_3O_4@Phenyl phosphate creatine. The TGA curve of the Fe_3O_4@Diphenyl phosphate creatine is shown in Figure 5. The sample lost 3.8% weight at below 130 °C that related to the loss of the adsorbed water. The TGA curve of the Fe_3O_4@Diphenyl phosphate creatine substrate shows weight loss between 130 °C and 400 °C which attributed to the decomposition of covalently bonded the organic groups (about 24.1%). Thus, the TGA curve proves the Fe_3O_4 functionalized with Phenyl phosphate creatine.

The nitrogen adsorption-desorption isotherms of Diphenyl phosphate creatine (curve 1), Fe_3O_4 (curve 2)

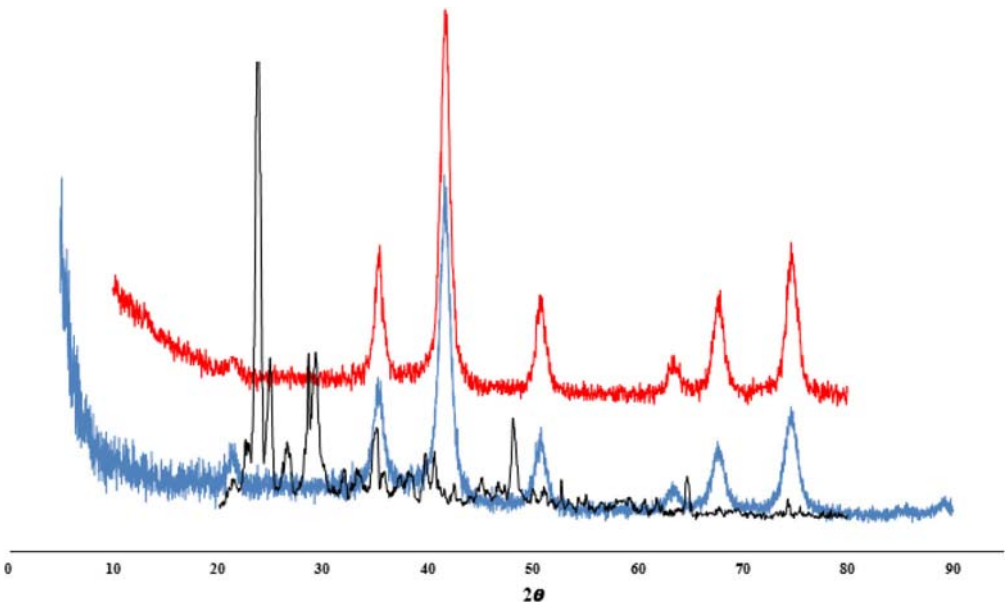

Figure 4. XRD patterns of Diphenyl phosphate creatine (Black curve), Fe_3O_4 (Red curve) and Fe_3O_4@Diphenyl phosphate creatine (Blue curve).

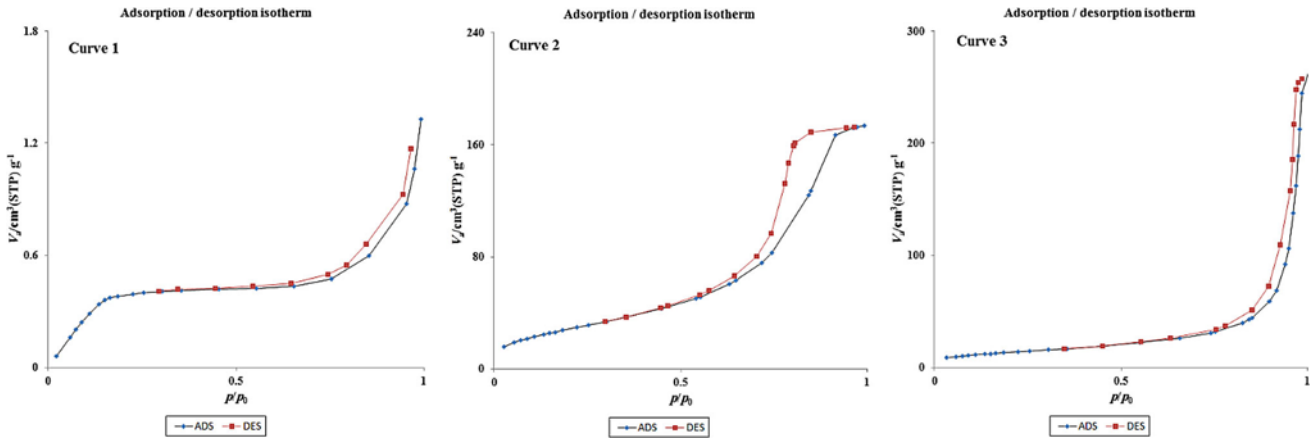

Figure 6. Nitrogen adsorption-desorption isotherms of Diphenyl phosphate creatine (curve 1), Fe_3O_4 (curve 2) and Fe_3O_4@Diphenyl phosphate creatine (curve 3).

Table 1. Optimization of the reaction temperature and the catalyst amounts.

Entry	Temperature (°C)	Amount of catalyst (mg)	Yield (%)
1	25[a]	50	35
2	50[a]	50	60
3	65[a]	50	70
4	70[a]	50	70
5	65[b]	–	30
6	65[b]	30	60
7	65[b]	40	65
8	65[b]	60	70

Reaction conditions: [a]5-substituted tetrazole derivatives (2 mmol) and α, β-unsaturated carbonyl (2 mmol) in methanol (10 mL) and the catalyst (50 mg) at different temperature. Reaction conditions: [b]5-substituted tetrazole derivatives (2 mmol) and α, β-unsaturated carbonyl (2 mmol) in methanol (10 mL) and a different amount of the catalyst at 65 °C.

Table 2. Screening of the catalysts.

Entry	Catalyst	Time (minute)	Yield (%)
1	–	60	35
2	Fe_3O_4	60	45
3	Fe_3O_4@Creatine	60	45
4	Fe_3O_4@Diphenyl phosphate creatine	60	70

Reaction conditions: 5-substituted tetrazole derivatives (2 mmol) and α, β-unsaturated carbonyl (2 mmol) in methanol (10 mL) and the catalyst (50 mg) at 65 °C.

and Fe_3O_4@Diphenyl phosphate creatine (curve 3) are exhibited in Figure 6. The corresponding parameters including BET surface area of the Fe_3O_4@Diphenyl phosphate creatine, Diphenyl phosphate creatine and Fe_3O_4 is 49.06 $m^2\ g^{-1}$, 1.1334 $m^2\ g^{-1}$ and 106.73 $m^2\ g^{-1}$ respectively. This observation suggests that with converting of homogenous catalyst to heterogeneous catalyst, the BET specific surface area of the catalyst is significantly increased.

3.1 *Investigation of catalytic activity of Fe_3O_4@Diphenyl phosphate creatine in the Aza-Michael reaction*

The catalytic potential of the Fe_3O_4@Diphenyl phosphate creatine after preparation and characterization was probed in the aza- Michael reaction. Initially, the blank experiment was optimized using the reaction between 5-(4-nitrophenyl)-1H-tetrazole and cyclohex-

Table 3. Fe_3O_4@Diphenyl phosphate creatine catalyzed the aza-Michael reaction.

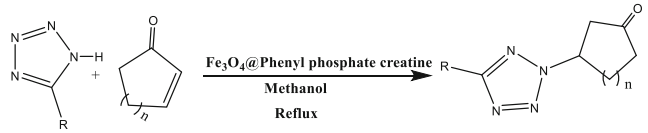

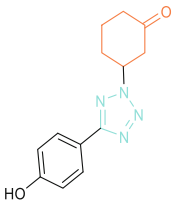

Compound 1, 55% yield, 95 min

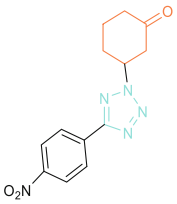

Compound 2, 70% yield, 60 min

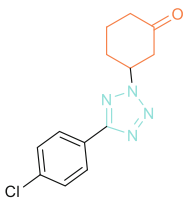

Compound 3, 70% yield, 180 min

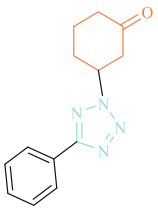

Compound 4, 85% yield, 60 min

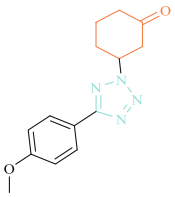

Compound 5, 70% yield, 85 min

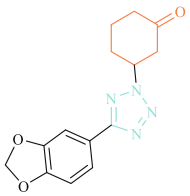

Compound 6, 65% yield, 80 min

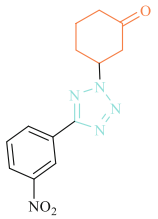

Compound 7, 85% yield, 70 min

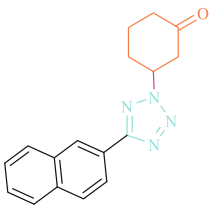

Compound 8, 20% yield, 130 min

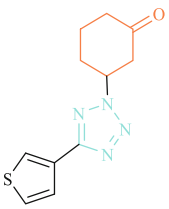

Compound 9, 55% yield, 85 min

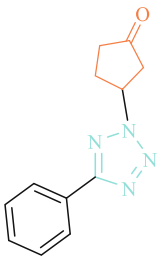

Compound 10, 65% yield, 90 min

Reaction conditions: 5-substituted tetrazole derivatives (2 mmol) and α, β-unsaturated carbonyl (2 mmol) in methanol (10 mL) and the catalyst (50 mg) at 65 °C.

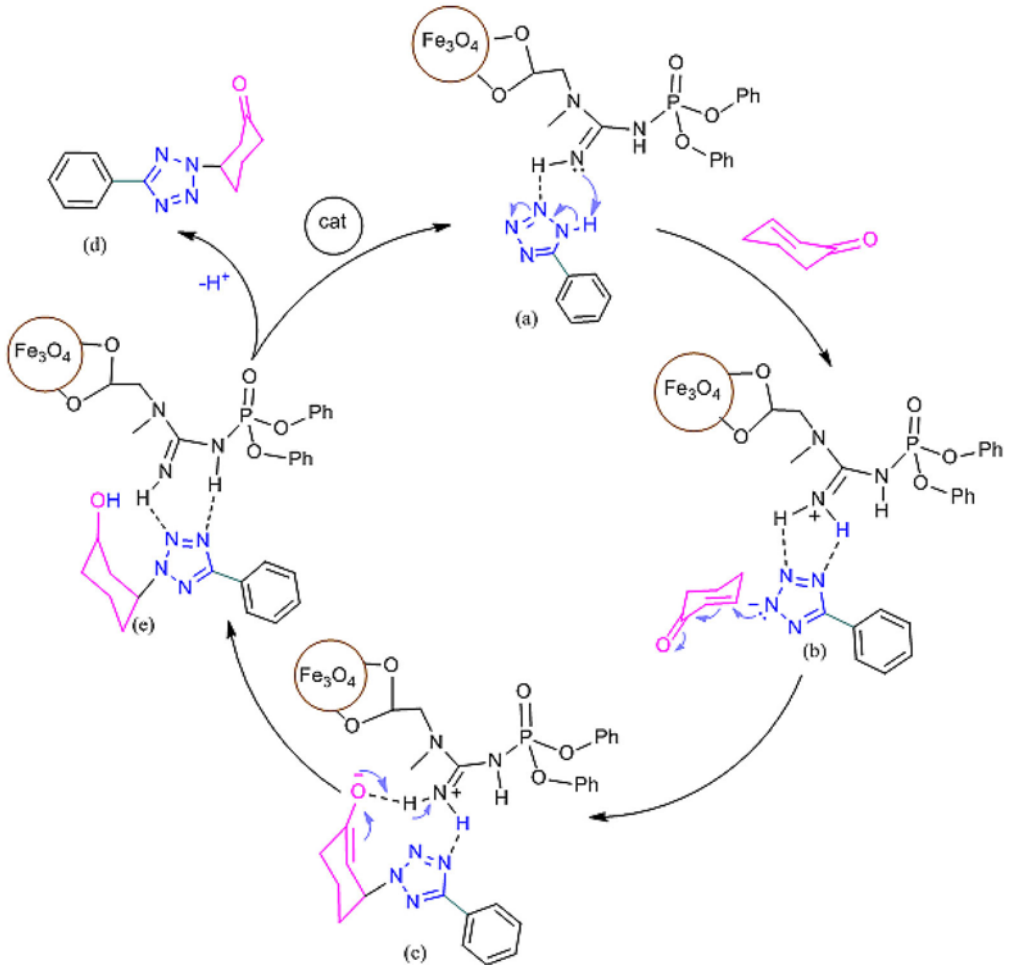

Scheme 2. Mechanism for the reaction between 5-substituted tetrazoles and α, β-unsaturated carbonyl in the presence of Fe_3O_4@Diphenyl phosphate creatine catalyst.

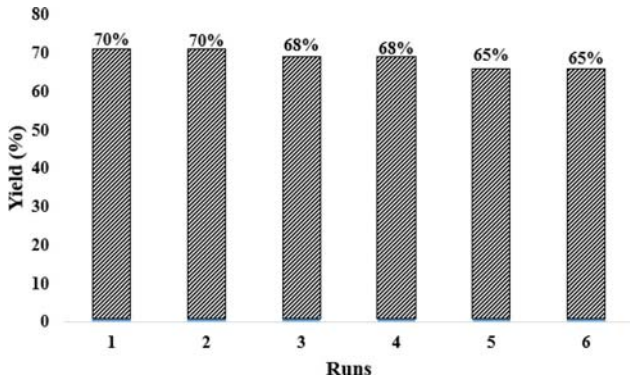

Figure 7. Catalyst reusability.

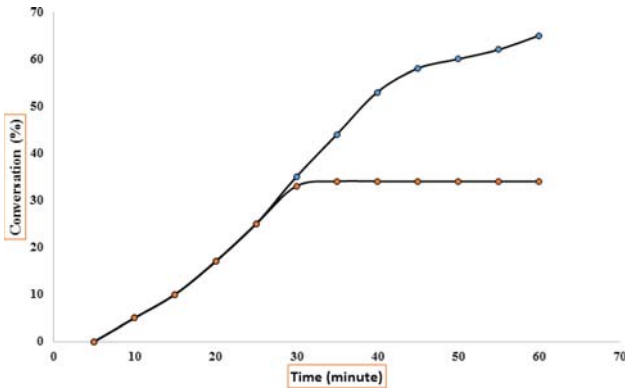

Figure 8. Leaching test for catalyst during a catalytic reaction.

2-enone as a model reaction in the presence of Fe_3O_4@Phenyl phosphate creatine. The reaction parameters including various catalyst amount and temperature were investigated to obtain maximum of the yield (Table 1). The corresponding aza- Micheal reaction was obtained at 35% yield at room temperature (Table 1, Entry 1) and by raising the temperature to 65 °C the product yield can be improved further (Table 1, Entry 3). Screening the amount of catalyst indicated that the reaction in 30 and 40 mg was sluggish to afford the desired product (Table 1, Entry 6 and 7). But it was found that 50 mg of Fe_3O_4@Diphenyl phosphate creatine gives the desired product. The model reaction was carried out with Fe_3O_4, Fe_3O_4@Diphenyl phosphate

creatine and in the absence of the catalyst. This reaction has low yield in the presence of Fe_3O_4 and Fe_3O_4@-Creatine and no product in the absence of the catalyst (Table 2, Entry 1 and 2).

We explored the catalytic activity of Fe_3O_4@-Diphenyl phosphate creatine for the aza-Michael reaction under the optimized reaction conditions. The reactions were performed by using different types of 5-substituted tetrazole and α, β-unsaturated carbonyl and the results are summarized in Table 3. It is observed that reactions between α, β-unsaturated carbonyl and 5-phenyl-2H-tetrazole or 5-(naphthalen-2-yl)-2H-tetrazole were provided in good yields (Table 3, Entry 4 and 7). But reaction α, β-unsaturated carbonyl between 5-(4-nitrophenyl)-2H-tetrazole or 5-(4-chlorophenyl)-2H-tetrazole gives moderate yields (Table 3, Entry 2 and 3). A probable mechanism for the aza-Michael reaction catalyzed with Fe_3O_4@Diphenyl phosphate creatine has been suggested in Scheme 2.

At first, the reaction of 5-substituted tetrazole with Fe_3O_4@Diphenyl phosphate creatine is expected to form the intermolecular hydrogen-bonded intermediate (a). Then nitrogen of tetrazole attacked to double bond of the α, β-unsaturated carbonyl (b) finally product was formed with the regeneration of the catalyst (d).

It was observed that the Fe_3O_4@Diphenyl phosphate creatine catalyst can be reused at least six times without significant loss in yields of the products (Figure 7).

We performed a leaching test to investigate the stability of the nanocomposite during the catalytic reaction (Figure 5). In the leaching test, the reaction was stopped after 4 h, and the catalyst was removed using a magnet. The reaction was further continued with the filtrate. However, after the stipulated time of 16 h, we did not observe any increment in product formation, which clearly suggests that no active species were leached during the course of the catalytic reaction.

Finally, the leaching test was carried out to investigate the stability of the nanoparticle during the catalytic reaction (Figure 8). After 30 min of reaction time, the catalyst was removed by using an external magnet and the solution was left to stir for 30 min. After that, the reaction had no progress which this shows that no active species were leached during the course of the catalytic reaction.

4. Conclusions

In summary, we successfully synthesized Fe_3O_4@-Diphenyl phosphate creatine as a highly efficient catalyst for the catalytic synthesis of tetrazole derivatives. A variety of 5-substituted tetrazoles reacted with α, β-unsaturated carbonyl in the presence of the catalyst affording the products in good yields. The magnetic organocatalyst is easily prepared and high specific surface, high stability, non-toxicity, low-cost, magnetically separation, easy recoverability and reusability are the main advantages of this unique nanocatalyst.

Supplementary Information (SI)

^{1}H NMR, ^{13}C NMR, and mass characterization data are available at www.ias.ac.in/chemsci.

Acknowledgements

The authors gratefully acknowledge the Faculty of Chemistry of Tarbiat Modares University for supporting this work.

References

1. Demko Z P and Sharpless K B 2002 An expedient route to the tetrazole analogues of α-amino acids *Org. Lett.* **4** 2525
2. Jin T, Kamijo S and Yamamoto Y 2004 Synthesis of 1-substituted tetrazoles via the acid-catalyzed [3 + 2] cycloaddition between isocyanides and trimethylsilyl azide *Tetrahedron Lett.* **45** 9435
3. Duncia J V, Pierce M E and Santella J B 1991 Three synthetic routes to a sterically hindered tetrazole. A new one-step mild conversion of an amide into a tetrazole *J. Org. Chem.* **56** 2395
4. Zhu Y, Ren Y and Cai C 2009 One-pot synthesis of 5-substituted 1H-tetrazoles from aryl bromides with potassium hexakis (cyano-κC)ferrate(4 −) (K4[Fe(CN)6]) as cyanide source *HCA* **92** 171
5. Montalbetti C A G N and Falque V 2005 Amide bond formation and peptide coupling *Tetrahedron* **61** 10827
6. Koldobskii G I 2006 Strategies and prospects in functionalization of tetrazoles *Russ. J. Org. Chem.* **42** 469
7. Bonollo S, Lanari D, Longo J M and Vaccaro L 2012 E-factor minimized protocols for the polystyryl-BEMP catalyzed conjugate additions of various nucleophiles to α,β-unsaturated carbonyl compounds *Green Chem.* **14** 164
8. Hayotsyan S S, Khachatryan A N, Baltayan A O, Attaryan H S and Hasratyan G V 2015 Addition of azoles to methyl vinyl ketone by the Aza-Michael reaction *Russ. J. Gen. Chem.* **85** 993
9. Madhavan N, Takatani T, Sherrill C and Weck M 2009 Macrocyclic cyclooctene-supported AlCl–salen catalysts for conjugated addition reactions: effect of linker and support structure on catalysis *Chem. Eur. J. Chem.* **15** 1186
10. Gandelman M and Jacobsen E N 2005 Highly enantioselective catalytic conjugate addition of

N-heterocycles to alpha,beta-unsaturated ketones and imides *Angew. Chem. Int. Ed. Engl.* **44** 2393
11. Tobias RFBG-HC 2007 Phosphoramidates and methods therefor U. S. Patent 7173020B2
12. Gholivand K, Kahnouji M, Mark Roe S, Gholami A and Fadaei F T 2017 Palladium (II) complexes of aminothiazole-based phosphines: synthesis, structural characterization, density functional theory calculations and catalytic application in heck reaction *Appl. Organomet. Chem.* **31** 3793
13. Gholivand K, Mohammadpanah F, Pooyan M, Valmoozi A A E, Sharifi M, Mani-Varnosfaderani A and Hosseini Z 2019 Synthesis, crystal structure, insecticidal activities, molecular docking and QSAR studies of some new phospho guanidines and phospho pyrazines as cholinesterase inhibitors *Pestic. Biochem. Phys.* **157** 122
14. Gholivand K, Asadi L, Valmoozi A A E, Hodaii M, Sharifi M, Kashani H M, Mahzouni H R, Ghadamyari M, Kalate A A and Davari E 2016 Phosphorhydrazide inhibitors: toxicological profile and antimicrobial evaluation assay, molecular modeling and QSAR study *RSC Adv.* **6** 24175
15. Gholivand K, Molaei F, Oroujzadeh N, Mobasseri R and Naderi-Manesh H 2014 Two novel Ag(I) complexes of N-nicotinyl phosphoric triamide derivatives: synthesis, X-ray crystal structure and in vitro antibacterial and cytotoxicity studies *Inorg. Chim. Acta* **423** 107
16. Arkel M, Garbati P, Salis A, Damonte G, Liessi N, Adriano E, Benatti U, Balestrino M and Millo E 2018 A novel method to synthesize phosphocreatine and phosphocreatine prodrugs *J. Med. Chem.* **14** 387
17. Ghosh R, Pradhan L, Devi Y P, Meena S, Tewari R, Kumar A, Sharma S, Gajbhiye N, Vatsa R and Pandey B N 2011 Induction heating studies of Fe_3O_4 magnetic nanoparticles capped with oleic acid and polyethylene glycol for hyperthermia *J. Mater. Chem.* **21** 13388
18. Zeng H, Li J, Wang Z, Liu J and Sun S 2004 Bimagnetic core/shell FePt/Fe_3O_4 nanoparticles *Nano. Lett.* **4** 187
19. Safaei-Ghomi J and Eshteghal F 2017 Nano-Fe_3O_4/PEG/succinic anhydride: a novel and efficient catalyst for the synthesis of benzoxanthenes under ultrasonic irradiation *Ultrason. Sonochem.* **38** 488
20. Naeimi H, Rashid Z, Zarnani A-H and Ghahremanzadeh R 2014 $MnFe_2O_4$@NH_2@2AB-Ni: a novel, highly active, stable and magnetically recoverable nanocatalyst and use of this heterogeneous catalyst in green synthesis of spirooxindoles in water *New. J. Chem.* **38** 5527
21. Amini A, Sayyahi S, Saghanezhad S J and Taheri N 2016 Integration of aqueous biphasic with magnetically recyclable systems: polyethylene glycol-grafted Fe_3O_4 nanoparticles catalyzed phenacyl synthesis in water *Catal. Commun.* **78** 11
22. Polshettiwar V, Luque R, Fihri A, Zhu H, Bouhrara M and Basset J M 2011 Magnetically recoverable nanocatalysts *Chem. Rev.* **111** 3036
23. Salamatmanesh A, Miraki M K, Yazdani E and Heydari A 2018 Copper (I)–caffeine complex immobilized on silica-coated magnetite nanoparticles: a recyclable and eco-friendly catalyst for click chemistry from organic halides and epoxides *Catal. Lett.* **148** 3257
24. Pazoki F, Mehraban J A, Shamsayei M, Bakhshi B, Esfandiarpour R, Miraki M K and Heydari A 2019 Aza-Michael addition of 5-substituted tetrazole catalysed by a novel nanoparticle solid base catalyst involving a layered zinc hydroxide supported on a ferrite core *ChemistrySelect* **4** 2568
25. Ghonchepour E, Yazdani E, Saberi D, Arefi M and Heydari A 2017 Preparation and characterization of copper chloride supported on citric acid-modified magnetite nanoparticles (Cu^{2+}-CA@ Fe_3O_4) and evaluation of its catalytic activity in the reduction of nitroarene compounds *Appl. Organomet. Chem.* **31** 3822
26. Sharma R K, Monga Y, Puri A and Gaba G 2013 Magnetite (Fe_3O_4) silica based organic-inorganic hybrid copper (ii) nanocatalyst: a platform for aerobic N-alkylation of amines *Green Chem.* **15** 2800